



CHORUS

This is the accepted manuscript made available via CHORUS. The article has been published as:

Suppression of Dephasing by Qubit Motion in Superconducting Circuits

D. V. Averin, K. Xu, Y. P. Zhong, C. Song, H. Wang, and Siyuan Han

Phys. Rev. Lett. **116**, 010501 — Published 8 January 2016

DOI: [10.1103/PhysRevLett.116.010501](https://doi.org/10.1103/PhysRevLett.116.010501)

Suppression of dephasing by qubit motion in superconducting circuits

D. V. Averin^{1,*}, K. Xu², Y. P. Zhong², C. Song², H. Wang^{2,†} and Siyuan Han^{3‡}

¹*Department of Physics and Astronomy, Stony Brook University, SUNY, Stony Brook, NY 11794-3800, USA*

²*Department of Physics, Zhejiang University, Hangzhou, Zhejiang 310027, China*

³*Department of Physics and Astronomy, University of Kansas, Lawrence, KS 66045, USA*

(Dated: December 9, 2015)

We suggest and demonstrate a protocol which suppresses the low-frequency dephasing by qubit motion, i.e., transfer of the logical qubit of information in a system of $n \geq 2$ physical qubits. The protocol requires only the nearest-neighbor coupling and is applicable to different qubit structures. Our analysis of its effectiveness against noises with arbitrary correlations, together with experiments using up to three superconducting qubits, show that for the realistic uncorrelated noises, qubit motion increases the dephasing time of the logical qubit as \sqrt{n} . In general, the protocol provides a diagnostic tool for measurements of the noise correlations.

Development of superconducting qubits [1–7] has reached the stage when it is interesting to discuss possible architectures of the quantum information processing circuits. The common feature of any quantum computation process of even moderate complexity is the requirement of information transfer between different elements of the qubit circuit. The most straightforward way of achieving this transfer is to physically move the quantum states representing the qubits of information along the circuit. In the case of superconducting qubits, potential for such a direct motion of logical qubits is offered by the so-called nSQUIDs [8, 9], but operation of these circuits in the quantum regime [10] still needs to be demonstrated experimentally. Another method of transferring logical qubits between different physical qubits, already developed in experiments and adopted in this work, is based on creating controlled qubit-qubit interaction through coupling to a common resonator bus [5, 11–13]. The goal of this work is to demonstrate that, in addition to its main function, transfer of information between different circuit elements designed to perform different functions, has an additional notable benefit: suppression of the low-frequency dephasing. We also show that it can be used to measure the noise correlations and, in this way, diagnose the primary sources of the noises.

The basic mechanism of the noise suppression by qubit motion relies on the fact that the low-frequency noise is typically produced by fluctuators - see, e.g., [14, 15], in the form of impurity charges or magnetic moments, localized in each individual physical qubit, and therefore, is not correlated among them. Motion of a logical qubit between different physical qubits limits the correlation time of the effective noise seen by this qubit, and therefore suppresses its decoherence rate. This effect is qualitatively similar to the motional narrowing of the NMR lines [16], with the main difference that it is based on the controlled transfer of the qubit state, not random thermal motion as in NMR. Our protocol also has some similarities to the dynamic decoupling schemes - see, e.g., [17, 18], where the qubit-noise interaction is suppressed by changing the qubit state in the effectively constant noise, while the

qubit motion achieves this by changing noise seen by the moving qubit state. Also, since the effectiveness of this mechanism is sensitive to the noise correlations not only in time, but in space, it can be used to investigate the distribution of the primary sources of noises in quantum circuits, promising a fast and reliable noise diagnostic tool and, ultimately, improving the circuit performance.

Quantitatively, we start with the basic model of dephasing in a system of n physical qubits, where each qubit is coupled to a source of Gaussian fluctuations $\xi_j(t)$, $j = 1, \dots, n$, of the energy difference between the computational basis states:

$$H_{dec} = -\frac{1}{2} \sum_{j=1}^n \sigma_j^z \xi_j(t),$$

$$\langle \xi_j(0) \xi_k(t) \rangle = \int \frac{d\omega}{2\pi} S_{j,k}(\omega) e^{-i\omega t}. \quad (1)$$

Here σ_j^z is the z Pauli matrix of the j th qubit, $S_{j,j}(\omega) \equiv S_j(\omega)$ - spectral density of noise $\xi_j(t)$ in the j th qubit, the terms $S_{j,k}(\omega)$, with $j \neq k$, account for the noise correlations in different qubits, and we set $\hbar = 1$. The qubits are assumed to be free, i.e., (1) is the only part of the system Hamiltonian that depends on the qubit variables.

If a logical qubit, $|\Psi\rangle = \alpha|0\rangle + \beta|1\rangle$, is prepared at time $t = 0$ as an initial state of the j th physical qubit and is kept there for a period τ , it will decohere due to the noise $\xi_j(t)$. This decoherence process can be characterized quantitatively by the function $F(\tau)$, defined as

$$F(\tau) = \frac{\sigma_j(\tau)}{\sigma_j(0)}, \quad \sigma_j(\tau) = \text{Tr}\{\sigma_j^+(\tau)\rho\}, \quad (2)$$

where ρ is the initial density matrix of the system, which consists of the qubit part and the part ρ_{env} describing the noise source:

$$\rho = |\Psi\rangle\langle\Psi|_j \otimes \prod_{k \neq j} |0\rangle\langle 0|_k \otimes \rho_{env}.$$

Time dependence of the raising Pauli matrix, $\sigma_j^+ = (\sigma_j^x + i\sigma_j^y)/2$, of the j th qubit is governed by the Heisenberg

equation of motion that follows from the Hamiltonian (1): $\dot{\sigma}_j^+(t) = -i\xi_j(t)\sigma_j^+(t)$, and gives, as usual,

$$\begin{aligned} F(\tau) &= \langle T \exp\{-i \int_0^\tau \xi_j(t) dt\} \rangle \\ &= \exp\{-\int_0^\tau dt \int_0^t dt' \langle \xi_j(t) \xi_j(t') \rangle\}. \end{aligned} \quad (3)$$

Here T denotes the time-ordering operator, and $\langle \dots \rangle$ – averaging over the noise source ρ_{env} . Experimentally, the function $F(\tau)$ is obtained by measuring the Ramsey fringes.

On the other hand, we can arrange the situation, when the logical qubit $|\Psi\rangle$, instead of staying just in one physical qubit for the entire time interval τ , is transferred successively from qubit 1 to qubit n spending the time τ/n in each of them, while the transfer processes themselves are done much faster than τ/n . Such transfers can be achieved, e.g., by applying SWAP gates to the successive pairs of physical qubits. Then, if the transfers are done accurately, so that the dephasing during them is negligible, the decoherence of the logical qubit $|\Psi\rangle$ in the total time τ is

$$\begin{aligned} F(\tau) &= \exp\left\{-\sum_{j=1}^n \int_0^{\tau/n} dt \int_0^t dt' \langle \xi_j(t) \xi_j(t') \rangle \right. \\ &\quad \left. - \sum_{j < k} \int_0^{\tau/n} dt dt' \left\langle \xi_k\left(\frac{\tau}{n}(k-j) + t\right) \xi_j(t') \right\rangle\right\}. \end{aligned} \quad (4)$$

If the noises are low-frequency and uncorrelated at different qubits, decoherence is suppressed with increasing number n of the physical qubits. Indeed, in this regime, it is appropriate to neglect the quantum part of the noise and the second sum in Eq. (4) which reduces to

$$F(\tau) = \exp\left\{-\frac{1}{\pi} \int d\omega \frac{\sin^2(\omega\tau/2n)}{\omega^2} \sum_{j=1}^n S_j(\omega)\right\}. \quad (5)$$

The low-frequency dephasing is obtained then by expanding sine in ω and keeping the first term:

$$F(\tau) = \exp\left\{-\frac{\tau^2}{2n^2} \sum_{j=1}^n W_j^2\right\}, \quad W_j^2 = \int_{\omega_l}^{\omega_h} \frac{d\omega}{2\pi} S_j(\omega). \quad (6)$$

For the experimentally relevant $1/f$ noise, $S_j(\omega) = A_j/|\omega|$, the last approximation applies directly if the high-frequency cutoff of the noise ω_h satisfies the condition $\tau/n \ll 1/\omega_h$. As shown in the Supplementary Material [19], even in the opposite regime, there are only weak logarithmic correction to scaling of the dephasing time with n , and the main conclusion remains the same. The low-frequency cutoff ω_l can be estimated as inverse of the time of the experiment, and $W_j^2 = (A_j/\pi) \ln(\omega_h/\omega_l)$. If all physical qubits have the same decoherence properties, $W_j = W$, we can rewrite Eq. (5) as

$$F(\tau) = e^{-(\tau/\tau_d)^2}, \quad \tau_d = \sqrt{2n}/W, \quad (7)$$

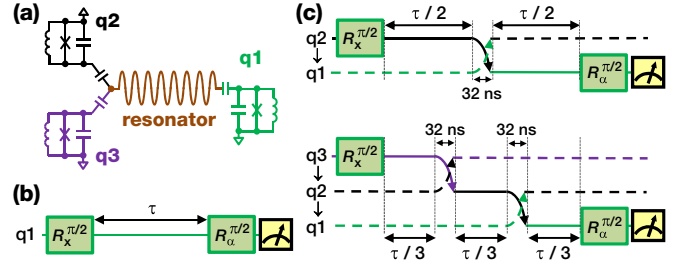


FIG. 1: (color online) (a) Device schematic showing three phase qubits capacitively coupled to a central resonator. (b) The experimental sequence of the Ramsey fringe measurement for a single qubit. (c) Experimental sequences for relaying the logical qubit state between two physical qubits (top) and among three physical qubits (bottom). The logical qubit moves along solid lines. The relay sequence starts with a $R_x^{\pi/2}$ rotation on the first qubit to create the logical qubit state in the $x-y$ plane of the Bloch sphere, i.e., $|\Psi\rangle = |0\rangle - i|1\rangle$. Relaying the logical qubit state to the next qubit is done by two successive qubit-resonator iSWAP gates that takes 32 ns in total (symbolized by the double crossed arrows). Finally a $R_\alpha^{\pi/2}$ rotation is applied to the last physical qubit in the sequence to bring the logical qubit state to the z -axis of the Bloch sphere for measuring the $|1\rangle$ -state probability of this qubit, P_1 . Here $\hat{\alpha}$ refers to the effective axis that rotates in the $x-y$ plane after removing the dynamical phase, i.e., $\hat{\alpha} = \cos(\omega_R\tau)\hat{x} + \sin(\omega_R\tau)\hat{y}$, where $\omega_R/2\pi$ is adjusted to around 25 MHz in the experiment.

and see that the dephasing time τ_d of the moving qubit increases in comparison to the stationary qubit as \sqrt{n} .

If the noises at different physical qubits are correlated, one needs to take into account both sums in Eq. (4). In this case, under the same assumptions as above, the dephasing time in Eq. (7) can be written as

$$\frac{1}{\tau_d^2} = \frac{1}{2n^2} \sum_{k,j=1}^n R_{k,j} = \frac{W^2}{2n^2} \left[n + 2 \sum_{j < k} r_{k,j} \right], \quad (8)$$

where $R_{k,j} \equiv \int d\omega S_{k,j}(\omega)/2\pi$. The second equality assumes that all qubits have the same noises $S_{j,j}(\omega) = S(\omega)$, with the coefficients $r_{k,j}$ defined in this case by the relation $S_{k,j}(\omega) = r_{k,j}S(\omega)$. They describe the degree of noise correlations between the k th and the j th qubit and have the property $|r_{k,j}| \leq 1$, with $r_{k,j} = 1$ corresponding to full correlations, and $r_{k,j} = -1$ describing full anticorrelations. Equation (8) shows that if all noises are fully correlated, then $\tau_d = \sqrt{2}/W$, and the qubit motion does not produce any suppression of dephasing.

To test experimentally the mechanism of dephasing suppression by qubit motion as discussed above, we perform the Ramsey fringe experiments (Fig. 1(b)) [20] using up to three superconducting qubits, among which the initial logical qubit state $|\Psi\rangle = |0\rangle - i|1\rangle$ (here and below we neglect the normalization constant) is relayed and its phase information is probed after the total relay time τ . We use two types of superconducting circuits in which dephasing noises differ very much in magnitude: one features three phase qubits, each capacitively coupled to a

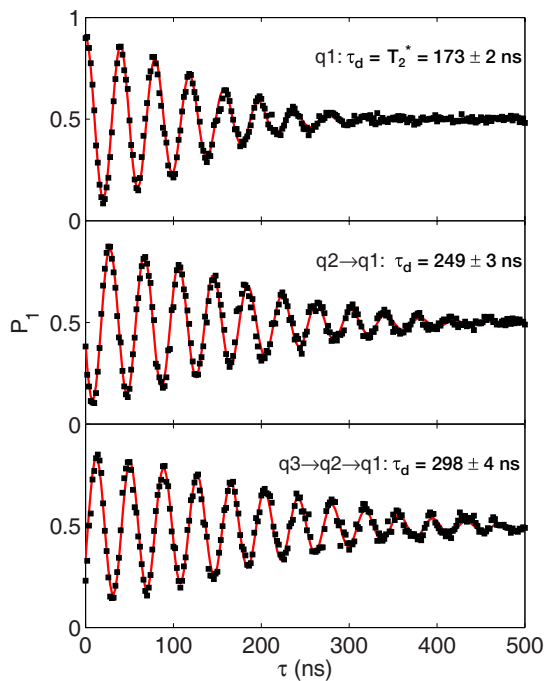


FIG. 2: (color online) The Ramsey fringe experimental data for sequences shown in Fig. 1. Red lines are fits according to Eq. (10). T_2^* for single qubit can be directly compared with τ_d for multiple qubits. Statistical errors, from the measured probability spread of $\sim 2\%$, are omitted for display clarity, but are used to estimate the standard deviations of T_2^* and τ_d .

common resonator [21, 22] (Fig. 1(a)), and the other one features two Xmon qubits with much reduced dephasing noises, each as well coupled capacitively to a common resonator. The Hamiltonian of these quantum circuits is

$$H = -\frac{1}{2} \sum_{j=1}^n \omega_j^q \sigma_j^z + \omega^r a^\dagger a + \sum_{j=1}^n \lambda_j (a \sigma_j^+ + a^\dagger \sigma_j^-), \quad (9)$$

where the resonator frequency ω^r and the qubit-resonator coupling strength λ_j ($\equiv \lambda$ under the homogeneous condition and $\ll \omega^r, \omega_j^q$) are fixed by the circuit design, and a^\dagger, a are the creation/annihilation operators of the resonator field. The qubit frequencies ω_j^q are individually tunable, and n ($= 1, 2$, or 3) is the total number of physical qubits involved in each experimental sequence.

For the phase qubit circuit, $\omega^r/2\pi = 6.22$ GHz and $\lambda/2\pi \approx 15.5$ MHz. The operation frequencies of qubits $q1$, $q2$, and $q3$ are chosen at 5.99, 6.04, and 6.06 GHz, respectively, for their dephasing times T_2^* to be about the same. Corresponding energy relaxation times T_1 are 512 ± 6 , 538 ± 6 , and 488 ± 4 ns. The dephasing times T_2^* s are 173 ± 2 , 177 ± 1 , and 176 ± 2 ns by fitting to $\ln[P_1(\tau)] \propto -\tau/2T_1 - (\tau/T_2^*)^2$, where P_1 is the $|1\rangle$ -state probability in the Ramsey fringe experiment [23]. Since three qubits have similar T_2^* values, we expect that the noise power spectral densities $S_j(\omega)$ ($j = 1, 2$, and 3),

which characterize the flux-noise environments of these qubits, are approximately at the same level [23–25].

At its operation frequency, each qubit is effectively decoupled from the resonator. If qubit $q1$ is in $|0\rangle - i|1\rangle$ and resonator r is in $|0\rangle$, we can turn on the qubit-resonator interaction by rapidly matching the qubit frequency to that of the resonator for a controlled amount of time, implementing an iSWAP gate [26] to transfer the state from $q1$ to resonator r , i.e., $(|0\rangle - i|1\rangle)_{q1}|0\rangle_r \rightarrow |0\rangle_{q1}(|0\rangle - |1\rangle)_r$. Immediately after the first iSWAP gate, we bring qubit $q2$, originally in $|0\rangle$, on resonance with the resonator r for another iSWAP gate. As such, other than a phase factor, we effectively relay the logical qubit state between the two qubits, i.e., $(|0\rangle - i|1\rangle)_{q1}|0\rangle_{q2} \rightarrow |0\rangle_{q1}(|0\rangle + i|1\rangle)_{q2}$ [22]. For the phase qubit circuit, an iSWAP gate takes about 16 ns and the total time for transferring the state from one qubit to the other qubit is about 32 ns.

We measure the Ramsey fringe of a logical qubit which spends equal amount of time in each of the $n \geq 2$ physical qubits. The sequences are illustrated in Fig. 1(c). The obtained Ramsey fringe is fitted according to [23]

$$P_1(\tau) = A \exp \left[-\frac{\tau}{2T_1^{ave}} - \frac{\tau^2}{\tau_d^2} \right] \cos(\omega_R \tau + B) + C, \quad (10)$$

where T_1^{ave} is fixed as the average of all qubits involved and τ_d is the effective dephasing time for the logical qubit as obtained from the fit (so are the constants A, B, C, and ω_R). Representative experimental data and fitting curves are shown in Fig. 2.

Controlled motion of the logical qubit is attempted under various experimental conditions. τ_d values obtained using different experimental sequences and different physical qubit combinations are listed in the Supplementary Material [19]. The Ramsey fringe measurements using two (three) phase qubits show that the dephasing times τ_d are extended to about 244.0 ± 3.1 ns (297.2 ± 5.5 ns), averaged a gain by a factor of $1.392 = 0.984\sqrt{2}$ ($1.695 = 0.979\sqrt{3}$) compared with those from the single-qubit measurements, 175.3 ± 2.3 ns. As expected from Eq. (5), the dephasing time τ_d of the logical qubit scales very well with the square root of the number of physical qubits, \sqrt{n} . The similar scaling is also observed using two Xmon qubits, where the single-qubit T_2^* values are about $1 \mu\text{s}$, achieving a gain of $1.405 = 0.993\sqrt{2}$ (Ramsey fringe data not shown). Our result clearly demonstrates that dephasing caused by uncorrelated low-frequency noises can be reduced by a factor of \sqrt{n} by moving the logical qubit along an array of $n \geq 2$ physical qubits.

In general, degree of the noise suppression by qubit motion method depends on the noise correlations. If the noises $S_j(\omega)$, $j = 1$ and 2 , for the two qubits are the same, we can express Eq. (8) as

$$\frac{1}{\tau_d^2} = \frac{W^2}{4} (1 + r_c), \quad \tau_d = \sqrt{\frac{2}{1 + r_c}} T_2^*, \quad (11)$$

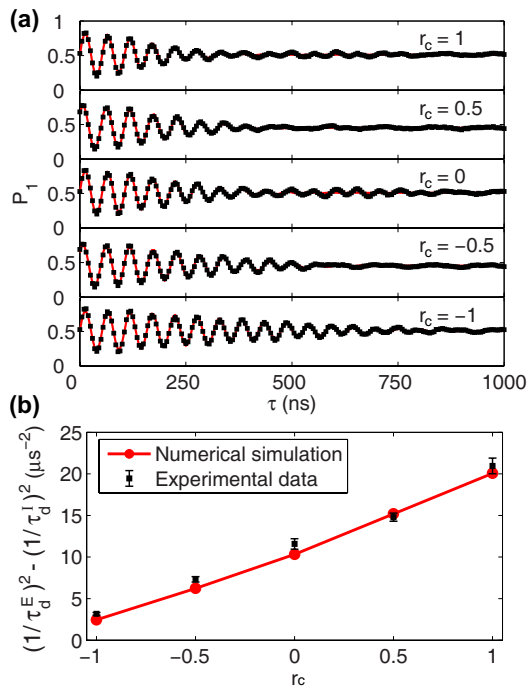


FIG. 3: (a) The 2-qubit Ramsey fringe results under artificial noises with different correlations r_c as indicated. Dots are experimental data and lines are fits. Fitted τ_d^E values are 213 ± 4 , 251 ± 4 , 281 ± 7 , 345 ± 6 , and 485 ± 8 ns from top to bottom. (b) $(1/\tau_d^E)^2 - (1/\tau_d^I)^2$ versus r_c (black squares), where τ_d^I is the dephasing time from the 2-qubit Ramsey fringe experiment under no artificial noise. Error bars are estimated based on uncertainties of τ_d^E and τ_d^I . The numerical result (red dots) is obtained by solving the Schrodinger-Langevin equation [29] with a time-dependent Hamiltonian, while the swap non-ideality is accounted for using the Lindblad master equation. Line is a guide to the eye.

where $T_2^* = \sqrt{2}/W$ and $r_c \equiv r_{1,2}$. The monotonous dependence of τ_d on the correlation coefficient r_c of the two-qubit noises provides a much needed tool for measuring noise correlations. Since the Ramsey fringe measurement is much faster than the conventional two-point correlation measurement [24, 27], Eq. (11) may provide a fast method for identifying the primary sources of noises in complex quantum circuits.

We experimentally emulate the monotonous dependence of τ_d on r_c in Eq. (11) using two Xmon qubits, where the much reduced intrinsic dephasing noises make it easier to inject controllable noises [28]. Here the intrinsic noises are any noises associated with the device or measurement setup, in contrast to the extrinsic ones that specifically refer to our controlled noises. We first set the operation frequencies of the two Xmon qubits, exposing them to the same level of intrinsic noise $S_j^I(\omega)$, $j = 1$ and 2 . We then apply strong low-frequency noises, digitally synthesized with an adjustable correlation coefficient r_c , to the two qubits so that their dephasing

rates are dominated by these extrinsic noises. It is verified that for each qubit T_2^* is reduced to about 220 ns due to the combination of the noise powers $S_j^I(\omega)$ and $S_j^E(\omega)$, $j = 1$ or 2 , where $S_j^E(\omega)$ are the synthesized noise power spectral densities (see Supplementary Material [19]). Synthesized noises are simultaneously applied during the 2-qubit Ramsey fringe experiments. Resulted Ramsey fringes shown in Fig. 3(a) can be used to estimate τ_d^E , the logic-qubit dephasing time determined by both $S_j^E(\omega)$ and $S_j^I(\omega)$, $j = 1$ and 2 . It is observed that τ_d^E increases monotonically when the correlation coefficient r_c changes from 1 to -1 , in agreement with Eq. (11). In Fig. 3(b), we plot $(1/\tau_d^E)^2 - (1/\tau_d^I)^2$ versus r_c (black squares with error bars), where τ_d^I is the logic-qubit dephasing time due only to $S_j^I(\omega)$, $j = 1$ and 2 , as measured with the 2-qubit Ramsey sequence without extrinsic noises. Also shown in Fig. 3(b) are the numerical simulation results. The experimental and simulation data are slightly different from the prediction by Eq. (11), likely due to the fact that experimentally synthesized extrinsic noises, limited by hardware resources, extend in frequency only down to 10 kHz.

To summarize, we propose and demonstrate a new scheme of suppression of the low-frequency dephasing of logical qubit based on its motion along an array of $n \geq 2$ physical qubits. The scheme is particular suited to quantum circuits which employ information transfer for their operation. Potential advantages of our approach include the possibility to make the physical qubit overhead insignificant by applying it to larger number of logical qubits. An array of n physical qubits can support the transfer of $n - 1$ independent logical qubits, with the dephasing time of all increased by motion as \sqrt{n} . It also should be straightforward to incorporate qubit motion into quantum gate operations on entangled logical qubits. Our results thus open a new venue for gaining insight into the low-frequency noises in complex quantum information processing circuits and for improving their performance.

The authors thank John Martinis for providing the devices used in the experiment. This work was supported by the National Basic Research Program of China (2014CB921200, 2012CB927404), US NSF grants PHY-1314758 and PHY-1314861, the National Natural Science Foundation of China (11434008, 11222437), and Zhejiang Provincial Natural Science Foundation of China (LR12A04001).

* Electronic address: dmitri.averin@stonybrook.edu

† Electronic address: hhwang@zju.edu.cn

‡ Electronic address: han@ku.edu

- [1] M. Neeley, R.C. Bialczak, M. Lenander, E. Lucero, M. Mariantoni, A.D. O'Connell, D. Sank, H. Wang, M. Weides, J. Wenner, Y. Yin, T. Yamamoto, A.N. Cleland, and J.M. Martinis, *Nature* **467**, 570 (2010).
- [2] L. DiCarlo, M.D. Reed, L. Sun, B.R. Johnson, J.M. Chow, J.M. Gambetta, L. Frunzio, S.M. Girvin, M.H. Devoret, and R.J. Schoelkopf, *Nature* **467**, 574 (2010).
- [3] H. Paik, D.I. Schuster, L.S. Bishop, G. Kirchmair, G. Catelani, A.P. Sears, B.R. Johnson, M.J. Reagor, L. Frunzio, L. I. Glazman, S.M. Girvin, M.H. Devoret and R.J. Schoelkopf, *Phys. Rev. Lett.* **107**, 240501 (2011).
- [4] J. Clarke and F.K. Wilhelm, *Nature* **453**, 1031 (2008).
- [5] M. Mariantoni, H. Wang, T. Yamamoto, M. Neeley, R.C. Bialczak, Y. Chen, M. Lenander, E. Lucero, A. D. O'Connell, D. Sank, M. Weides, J. Wenner, Y. Yin, J. Zhao, A.N. Korotkov, A.N. Cleland and J.M. Martinis, *Science* **334**, 61 (2011).
- [6] A. Fedorov, L. Steffen, M. Baur, M.P. da Silva and A. Wallraff, *Nature* **481**, 170 (2012).
- [7] J. Kelly, R. Barends, A. G. Fowler, A. Megrant, E. Jeffrey, T.C. White, D. Sank, J. Y. Mutus, B. Campbell, Y. Chen, Z. Chen, B. Chiaro, A. Dunsworth, I.C. Hoi, C. Neill, P.J.J. O'Malley, C. Quintana, P. Roushan, A. Vainsencher, J. Wenner, A.N. Cleland and J.M. Martinis, *Nature* **519**, 66 (2015).
- [8] V.K. Semenov, G.V. Danilov, and D.V. Averin, *IEEE Trans. Appl. Supecond.* **13**, 938 (2003).
- [9] J. Ren, V.K. Semenov, Yu.A. Polyakov, D.V. Averin, and J.-S. Tsai, *IEEE Trans. Appl. Supecond.* **19**, 961 (2009).
- [10] Q. Deng and D.V. Averin, *J. Exp. Theor. Phys.* **119**, 1152 (2014).
- [11] M.A. Sillanpää, J.I. Park, and R.W. Simmonds, *Nature* **449**, 438 (2007).
- [12] J. Majer, J.M. Chow, J.M. Gambetta, J. Koch, B.R. Johnson, J.A. Schreier, L. Frunzio, D.I. Schuster, A.A. Houck, A. Wallraff, A. Blais, M.H. Devoret, S.M. Girvin and R.J. Schoelkopf, *Nature* **449**, 443 (2007).
- [13] C.-P. Yang, Q.-P. Su, S.-B. Zheng, and S. Han, *Phys. Rev. B* **92**, 054509 (2015).
- [14] O. Astafiev, Yu.A. Pashkin, Y. Nakamura, T. Yamamoto, and J.S. Tsai, *Phys. Rev. Lett.* **93**, 267007 (2004).
- [15] S. Sendelbach, D. Hover, M. Mueck, and R. McDermott, *Phys. Rev. Lett.* **103**, 117001 (2009).
- [16] C. Kittel, *Introduction to solid-state physics*, (Wiley, 1996), Ch. 16.
- [17] G.S. Uhrig, *Phys. Rev. Lett.* **98**, 100504 (2007).
- [18] J. Bylander, S. Gustavsson, F. Yan, F. Yoshihara, K. Harrabi, G. Fitch, D.G. Cory, Y. Nakamura, J.-S. Tsai and W.D. Oliver, *Nat. Phys.* **7**, 565 (2011).
- [19] Supplementary Material at <http://link.aps.org/supplemental/...>, which includes Refs. [30–32].
- [20] I. Chiorescu, Y. Nakamura, C.J.P.M. Harmans, J.E. Mooij, *Science* **299**, 1869 (2003).
- [21] E. Lucero, R. Barends, Y. Chen, J. Kelly, M. Mariantoni, A. Megrant, P. O'Malley, D. Sank, A. Vainsencher, J. Wenner, T. White, Y. Yin, A.N. Cleland and J.M. Martinis, *Nat. Phys.* **8**, 719 (2012).
- [22] Y.P. Zhong, Z.L. Wang, J.M. Martinis, A.N. Cleland, A.N. Korotkov and H. Wang, *Nat. Commun.* **5**, 3135 (2014).
- [23] D. Sank, R. Barends, R.C. Bialczak, Y. Chen, J. Kelly, M. Lenander, E. Lucero, M. Mariantoni, A. Megrant, M. Neeley, P. J. J. O'Malley, A. Vainsencher, H. Wang, J. Wenner, T.C. White, T. Yamamoto, Y. Yin, A.N. Cleland and J.M. Martinis, *Phys. Rev. Lett.* **109**, 067001 (2012).
- [24] F. Yan, J. Bylander, S. Gustavsson, F. Yoshihara, K. Harrabi, D.G. Cory, T.P. Orlando, Y. Nakamura, J.-S. Tsai and W.D. Oliver, *Phys. Rev. B* **85**, 174521 (2012).
- [25] F. Yoshihara, Y. Nakamura, F. Yan, S. Gustavsson, J. Bylander, W.D. Oliver and J.-S. Tsai, *Phys. Rev. B* **89**, 020503(R) (2014).
- [26] M. Neeley, M. Ansmann, R.C. Bialczak, M. Hofheinz, N. Katz, E. Lucero, A. O'Connell, H. Wang, A.N. Cleland and J.M. Martinis, *Nat. Phys.* **4**, 523 (2008).
- [27] R.C. Bialczak, R. McDermott, M. Ansmann, M. Hofheinz, N. Katz, E. Lucero, M. Neeley, A.D. O'Connell, H. Wang, A. N. Cleland and J.M. Martinis, *Phys. Rev. Lett.* **99**, 187006 (2007).
- [28] M.J. Biercuk, H. Uys, A.P. VanDevender, N. Shiga, W. M. Itano and J.J. Bollinger, *Nature* **458**, 996 (2009).
- [29] K. Yasue, *Ann. Phys.* **114**, 479 (1978).
- [30] M. Neeley, M. Ansmann, R.C. Bialczak, M. Hofheinz, N. Katz, E. Lucero, A. O'Connell, H. Wang, A.N. Cleland, and J.M. Martinis, *Phys. Rev. B* **77** 180508 (2008).
- [31] J.M. Martinis, *Quant. Inf. Proc.* **8**, 81 (2009).
- [32] R. Barends, J. Kelly, A. Megrant, D. Sank, E. Jeffrey, Y. Chen, Y. Yin, B. Chiaro, J. Mutus, C. Neill, P. O'Malley, P. Roushan, J. Wenner, T.C. White, A.N. Cleland, and J.M. Martinis, *Phys. Rev. Lett.* **111** 080502 (2013).